A Novel Planar Switched Reluctance Motor for Industrial Applications

J. F. Pan[1], N. C. Cheung[1], W. C. Gan[2], and S. W. Zhao[1]

[1]Department of Electrical Engineering, Hong Kong Polytechnic University, Kowloon, Hong Kong
[2]ASM Assembly Automation Hong Kong Ltd., Hong Kong

This paper presents a novel two-dimensional (2-D) planar switched reluctance motor (PSRM) for position control applications. The proposed 2-D planar motor has the advantages of simple mechanical construction, high reliability, and the ability to withstand hostile operating conditions. Due to the unique structure of the planar motor's magnetic circuit, there is very little coupling between the X- and Z-axis, and no decoupling compensation is needed. It is expected that this innovative SR planar motion system will be an ideal replacement for traditional X-Y tables in industrial automation applications.

Index Terms—**Planar motor, switched reluctance, X-Y table.**

I. Introduction

MODERN industrial applications often require precise two-dimensional (2-D) motions such as part assembly and component insertion. Traditional X-Y tables using rotary motors with mechanical transmissions stacked on top of each other have high cost, reduced accuracy, complex mechanical structure, and frequent maintenance. Therefore, direct-drive systems are expected to replace the rotary-to-linear methods to achieve linear/planar motions.

The Sawyer motor [1] is the first type of machine providing two axes of movement and the only sort of planar motor available to industry. Though it can provide uniform performance over the entire workspace and offers high speed, its open-loop stepping manner often leads to loss of steps and performance deterioration from external disturbances. The next generation of planar machines operating under closed-loop mode is mostly a permanent magnet type of motor, since 2-D motion from induction motors is difficult to achieve due to the complicated configuration of the core structure [2]. However, no matter where the permanent magnets are located, the designers will always encounter the problems of either complex stator coil structure [3] or massive expenses spent on large number of N-pole and S-pole permanent magnetic blocks [4].

Therefore, we propose a 2-D direct-drive, low-cost, easy-to-manufacture machine based on the switched reluctance principle for prospective industrial applications. This motor consists of the following major components:

1) aluminum base with multiple, laminated silicon-steel (Si-steel) blocks;
2) six laminated Si-steel slots wound with coils with an arrangement such that any one slot and its adjacent neighbors are responsible for different axes of motion;
3) two pairs of supporting mechanical slides holding the moving platforms and maintaining the air-gap;
4) optical encoders mounted on each moving platform to detect and feedback its real-time position information.

TABLE I
Motor Specifications

Symbol	Parameter	Value
Mx	Mover mass (X)	8.75 Kg
My	Mover mass (Y)	15 Kg
S	Size of base plate	450×450 mm
l	Travel distance	300×300 mm
z	Air gap	0.55 mm
N	Number of turns per phase	160 N
R	Phase resistance	1.5 Ω
p	Pole pitch	6 mm
d	Pole width	6 mm
q	Pole slot	6 mm
u	Encoder precision	0.5 μm

The purpose of this paper is to characterize and provide a thorough analysis on the motor's structure. The paper is arranged as follows. Its design and construction are introduced in Section II. Relative formulations for the motion system are given in Section III. Section IV focuses on the features of the motor and corresponding finite-element method (FEM) analysis and experimental results are provided. Concluding remarks are given in Section V.

II. Machine Construction

This motor derives from a former design of a linear switched reluctance motor (LSRM) built in our laboratory with accurate position control of 1 μm of precision [5]. The planar motor incorporates the design advantages of the previous LSRM for precise 2-D position control applications. Table I summarizes its main mechanical parameters.

The planar switched reluctance motor (PSRM) is a natural continuation from the previous idea with the extension of movements into two dimensions. The motor structure applies

Digital Object Identifier 10.1109/TMAG.2006.879143

0018-9464/$20.00 © 2006 IEEE

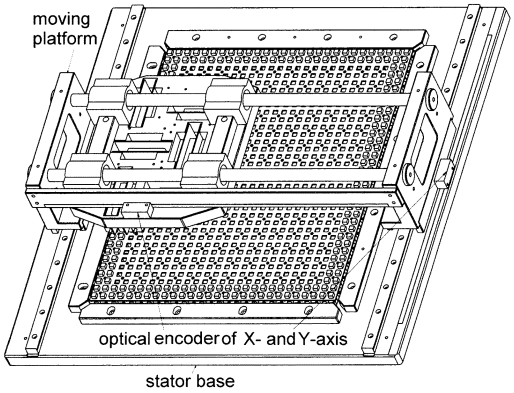

Fig. 1. Motor structure.

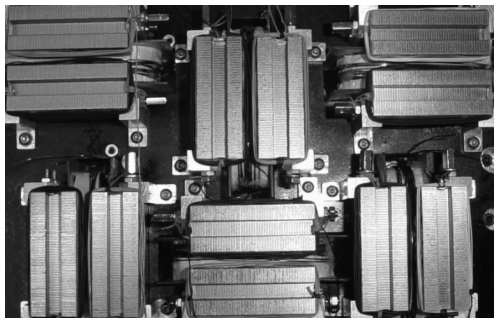

Fig. 2. Structure of the moving platform.

the "passive stator–active translator" scheme for the following reasons:

1) simple manufacturing of the stator base with no complicated coil arrays;
2) flexible traveling range and stator dimensions;
3) easy manufacture of mover slots with mounted coil windings;
4) low overall production cost.

Fig. 1 shows the overall structure.

A. Mover Structure

The moving platform consists of two sets of three-phase windings. Coils for perpendicular force generation are arranged in alternation and mounted on the mover slots with wide magnetic teeth (Fig. 2). All six movers together with windings have the same dimensions and ratings. The arrangement has the following features and advantages [6]:

1) the individual mover slot with coil simplifies the winding scheme, and thus, reduces the manufacturing cost of the moving platform;
2) zero mutual inductance can be achieved between adjacent movers with flux-decoupled windings [7];
3) long travel distance can be accomplished easily with the combination of longitudinal tracking supports.

B. Stator Structure

The stator contains multiple laminated Si-steel blocks held together by epoxy glue, a rigid aluminum base plate to support them firmly fixed, and sliding supports to hold the platform and maintain the air-gap. Instead of fabricating the stator base from a slab of sheet, this machine uses the *LEGO* block idea [8]. The stator is constructed from the combinations of magnetic blocks. The block elements are laminated with 0.5 mm Si-steel plates and all have the same dimensions. The art of stator structure is the "building blocks" approach that each block connects with another to comprise one unit of stator (Fig. 3). Next, any number of such units can be combined together to form a whole base as needed. This unique stator structure not only reduces eddy currents, but the "building element" concept makes mass production and flexible modifications of any size feasible starting from one piece, thus, drastically reducing the overall construction complexity and manufacturing cost.

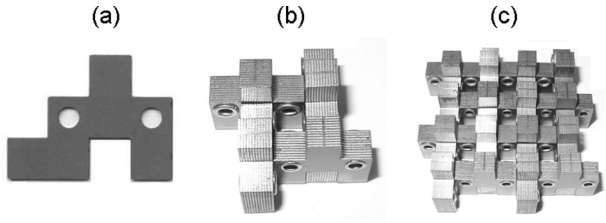

Fig. 3. Formation of the stator. (a) Single stator plate. (b) Building blocks. (c) One stator expansion.

From the perspective view of decoupled movements, the thickness of each mover is chosen to be a multiple of the stator pole-pitch to ensure unchanged overlap air-gap area and effective magnetic circuit wherever the moving platform resides according to current excited coil(s) [6]. The supporting guides are responsible to overcome the attraction force and maintain a uniform air-gap space. Since the positions of the platform are detected by the optical encoders and the positional errors can be corrected in real time, the uneven air-gap distribution will not impose a big problem to the motor. Furthermore, due to the short magnetic circuit paths of the flux-decoupled coils on the moving platform, the slight gaps among the stator blocks have a negligible effect on the overall performance of the planar motor, since proper control schemes will be applied to overcome manufacturing flaws. Therefore, the working accuracy is not dependent on the mechanical accuracy, but on the applied control algorithms.

III. System Formulation

The equations that govern the entire system model can be described in state-space as follows [7]:

$$\dot{I}_k = \frac{1}{L_k}\left(U_k - (R_k + \frac{\partial L_k}{\partial s_{x(y)}} \cdot v_{x(y)})\right) I_k \tag{1}$$

$$\dot{v}_{x(y)} = (F_{x(y)} - B_{x(y)} V_{x(y)} - F_{Lx(y)})/M_{x(y)} \tag{2}$$

$$\dot{s}_{x(y)} = v_{x(y)} \tag{3}$$

where U_k and I_k are the input voltage and current vectors for the kth coil ($k = 1$–6). $M_{x(y)}$, $F_{(x,y)}$, $B_{(x,y)}$, $v_{(x,y)}$, and $F_{L(x,y)}$ are mass, electromagnetic force, friction coefficient, velocity, and load vector, respectively, for the X- and Y-axis of movement. s_x and s_y are the displacement vector for the X- and Y-axis, respectively. R_k and L_k are a 6×6 diagonal matrix since mutual inductance between any movers is zero.

TABLE II
CALCULATION OF FORCE FROM (1) THEORETICAL METHOD AND (2) EXPERIMENT AT 8A WITHIN HALF POLE-PITCH

pos	0	0.93	1.06	1.59	2.48	3.11	3.51	4.01	4.43	5.09	5.5	5.99
1	0	-14.11	-15.89	-22.31	-29.05	-30.11	-29.09	-26.04	-22.09	-13.83	-7.81	-0.16
2	0	-15.87	-16.60	-19.18	-21.68	-23.01	-22.74	-21.35	-18.93	-13.60	-9.58	0.15

Self-inductance for any of the six coils can be expressed in Fourier series by taking the first-order approximation [9]

$$L_a = L_{\rm ls} + L_o + L_\Delta \cos\left(\frac{2\pi s_{x(y)}}{p}\right) \tag{4}$$

$$L_b = L_{\rm ls} + L_o + L_\Delta \cos\left(\frac{2\pi s_{x(y)} - \frac{2}{3}\pi p)}{p}\right) \tag{5}$$

$$L_c = L_{\rm ls} + L_o + L_\Delta \cos\left(\frac{2\pi s_{x(y)} - \frac{4}{3}\pi p)}{p}\right) \tag{6}$$

where

$$L_o = \frac{\mu_0 d^2 N^2}{z} \cdot \frac{p-q}{p} \tag{7}$$

$$L_\Delta \approx \frac{\mu_0 d^2 N^2}{z} \cdot \frac{q}{p} \tag{8}$$

and L_{ls} is the leakage inductance.

Force is calculated as the change of co-energy $W_{\rm co}$ according to displacement as follows:

$$F_{x(y)} = \frac{\partial W_{\rm co}}{\partial s_{x(y)}}. \tag{9}$$

If the motor is operated under unsaturated region

$$F_{x(y)} = \frac{1}{2}\frac{\partial L_k}{\partial s_{x(y)}} I_k^2. \tag{10}$$

Values of force comparisons at 8A are provided in Table II.

IV. CHARACTERISTICS VERIFICATION

To precisely represent the model in finite-element (FE) analysis, three-dimensional models have been constructed so that spatial phenomena such as the fringing effect can be fully explored. Then corresponding experimental measurements have been carried out to verify the simulated results with the FEM package *MEGA* from Bath University, U.K.

A. Mutual Inductance Effect

A mover with its closest neighbor is chosen to inspect the couplings. Intuitively, the magnetic field merely distributes within the short magnetic path among the movers with its excitation coil at 8A, the stator area and the air-gap space between them. This is because the magnetic path between the two adjacent movers has relatively large reluctances. An experiment on the mutual effect has already been carried out in [6] and detailed results are given. The numerical results from FEM for the flux distribution from each air-gap space of the two movers show that coupling effects among any of the six movers are negligible [Fig. 4(a) and (b)].

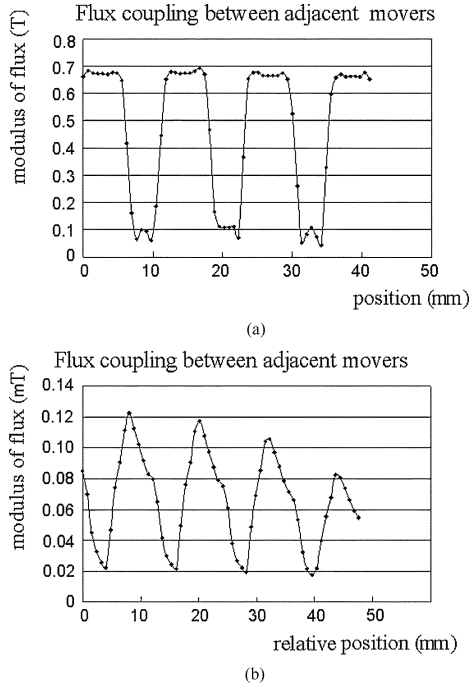

Fig. 4. Flux distribution when one mover is activated (8A). (a) Mover1. (b) Mover2.

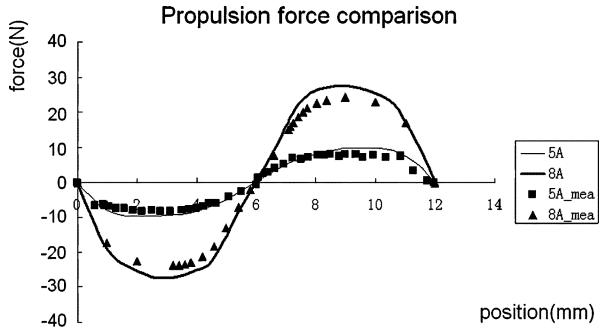

Fig. 5. Propulsion force from FEM and experimental results at 5A and 8A.

B. Single Force Output

Since movers are flux-decoupled from each other, only one mover with enough stator scope and air region is sufficient for FE models. Different current values are input to the coil winding and force is calculated at every movement. For direct force measurement, the force is measured from the load-cell mounted on the mover and force information is fed back to the computer [6]. The results from FEM and experiment are drawn in the same picture (Fig. 5). The unevenly distributed force output may come from: 1) A slight change of air-gap distance between the mover and stator during current excitation or 2) static friction forces. Overall, the data from FEM and experiment correlate with each other satisfactorily.

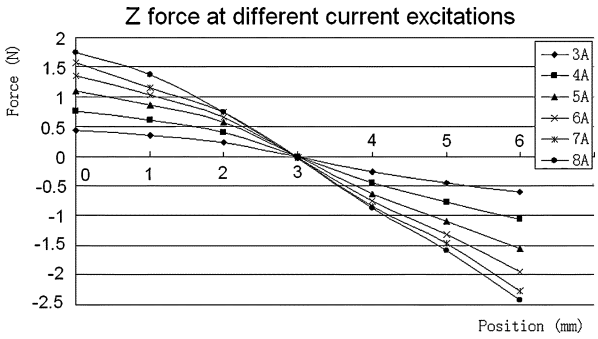

Fig. 6. Force disparities along Z-axis at fixed X position (X = 3 mm).

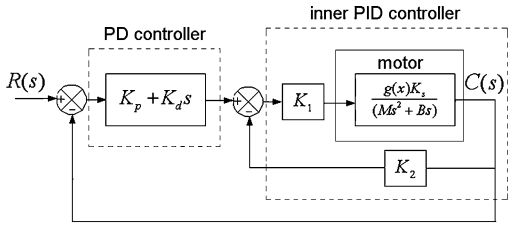

Fig. 7. Control diagram.

C. Force Disparity in Z-Axis

Last is the analysis of force disparity in the same X position according to different Z positions. Fig. 6 shows force variations according to the Z direction. There is a certain amount of force shifts for different Z positions, however, this influence is minor and, therefore, there is no need for any compensation from the control schemes.

V. Experimental Results

To further observe the motor performance under real operations, an improved dual-loop proportional-integral- derivative (PID) control scheme is proposed, as a complement of [6]. Fig. 7 shows the control diagram.

The experiment is conducted with the aim to verify the motor tracking capability under independently controlled manner. Both axes of motion apply the same control scheme proposed in Fig. 7 with slight parameter modifications according to different physical values such as mass or friction coefficient. With each position command as *sine* and *cosine* signals, the motor will move as a circle.

The controller is implemented with a dSPACE DS1104 controller card with a digital signal processor (DSP) clock frequency of 250 MHz. A PC interfaces with it through a PCI bus. The position feedback signal is collected by optical encoders attached to each mover and the reference current is generated by the controller card and passed to the digital-to-analog converters (DACs) and delivered to current drivers of the motor. The current signal is sensed by current transducers and fed back to the DSP through the analog-to-digital converters (ADCs).

The experimental result in Fig. 8 demonstrates that the motor is capable of tracking the compound command signal precisely so that the waveform of the command and response almost overlap. Therefore, it is suitable for industrial applications where 2-D movements with high precision are greatly required, such as component insertion and part assembly.

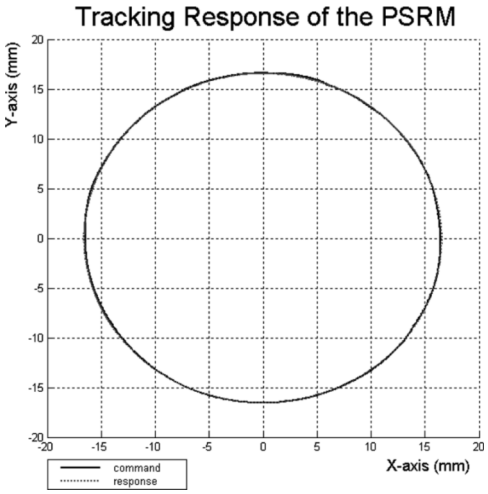

Fig. 8. Dynamic performance of the PSRM.

VI. Conclusion

The development of a 2-D motion system based on the SR principle has been described in this paper. The motor has a very simple and flexible structure. The motor consists of a moving platform which houses six coil windings that can be made by a coil winding machine individually. The base plate is constructed from small pieces of laminated blocks which can be mass produced cheaply and easily. Moreover, there is no need for costly and difficult-to-handle motor components, such as magnets, commutators, or complex overlap windings. Preliminary analysis and experiments show that the motion system has good characteristics and is suitable for precise position control applications. It is expected that the new motion system will be an ideal replacement for traditional X-Y tables to achieve equal precision performance.

Acknowledgment

This work was supported by the Hong Kong Polytechnic University Research Grants Council under the project code B-Q473.

References

[1] E. Pelta, "Two-axis Sawyer motor for motion systems," *IEEE Control Syst. Mag.*, vol. 7, no. 5, pp. 20–24, Oct. 1987.
[2] N. Fujii and T. Kihara, "Surface induction motor for two dimensional drive," *Trans. IEE Jpn.*, pt. D, vol. 118-D, no. 2, pp. 221–228, Feb. 1998.
[3] A. F. Flores Filho, A. A. Susin, and M. A. da Sliveira, "Development of a novel planar actuator," in *Proc. 9th Int. Conf. Electrical Machines and Drives*, Sep. 1999, pp. 268–271. Conf. Publ. no. 468.
[4] D. Ebihara and M. Watada, "Study of a basic structure of surface actuator," *IEEE Trans. Magn.*, vol. 25, no. 5, pp. 3916–3918, Sep. 1989.
[5] W.-C. Gan, N. C. Cheung, and L. Qiu, "Position control of linear switched reluctance motors for high-precision applications," *IEEE Trans. Ind. Appl.*, vol. 39, no. 5, pp. 1350–1362, Sep.–Oct. 2003.
[6] J. F. Pan, N. C Cheung, and J. Yang, "High-precision position control of a novel planar switched reluctance motor," *IEEE Trans. Ind. Electron.*, vol. 52, no. 6, pp. 1644–1652, Dec. 2005.
[7] C.-T. Liu and J.-L. Kuo, "Experimental investigation and 3-D modeling of linear variable-reluctance machine with magnetic-flux decoupled windings," *IEEE Trans. Magn.*, pt. 1–2, vol. 30, no. 6, pp. 4737–4739, Nov. 1994.
[8] N. C. Cheung, J. F. Pan, and J. M. Yang, "Two dimensional variable reluctance planar motor," U.S. Patent, Ref. IP-135A, file no. I040420E, filed July 2004.
[9] F. Khorrami, P. Krishnamurthy, and H. Melkote, *Modeling and Adaptive Nonlinear Control of Electric Motors*. New York: Springer, 2003.

Manuscript received March 8, 2006; revised May 9, 2006 (e-mail: daniel.pan@polyu.edu.hk).